Supporting Information

Deactivation Pathways of Neutral Ni(II) Polymerization Catalysts

*Andreas Berkefeld and Stefan Mecking**

University of Konstanz, Chair of Chemical Materials Science, Department of Chemistry,

Universitätsstrasse 10, D-78457 Konstanz, Germany

E-mail: stefan.mecking@uni-konstanz.de

General reactivity of neutral Ni(II)-methyl complexes.

A 9.8 mM solution of **1-DMSO** in CD_2Cl_2 was prepared at room temperature and stored at -30°C. In general, samples of **1-DMSO** in non coordinating solvents should not be kept at ambient temperatures for prolonged times since gradual decomposition to ethane occurs. ^{1}H NMR spectra were acquired at -60°C, -20°C, 0°C, 25°C, 35°C and 45°C. Figure S1 shows the ^{1}H NMR spectrum obtained at -20°C. In general, the line widths of the [(N,O)NiC*H*$_3$(DMSO)] and [(N,O)NiCH$_3$(*DMSO*)] resonances increased upon warming the sample to temperatures above 25°C. Furthermore, the resonance of free DMSO was observed to shift continuously from 2.55 ppm at T < 0°C to 3.24 ppm at T > 25°C. The equilibrium constants $K_{Me}(T)$ = **[1-DMSO]**$_{trans}$/**[1-DMSO]**$_{cis}$ were determined directly from the NMR spectra by integration of the Ni(II)-C*H*$_3$ resonances. Figure S2 depicts the plot of ln($K_{Me}(T)$) versus 1/T, providing the reaction enthalpy and entropy from which the free enthalpy difference between the *trans* and the *cis* isomer of **1-DMSO** was calculated for room temperature.

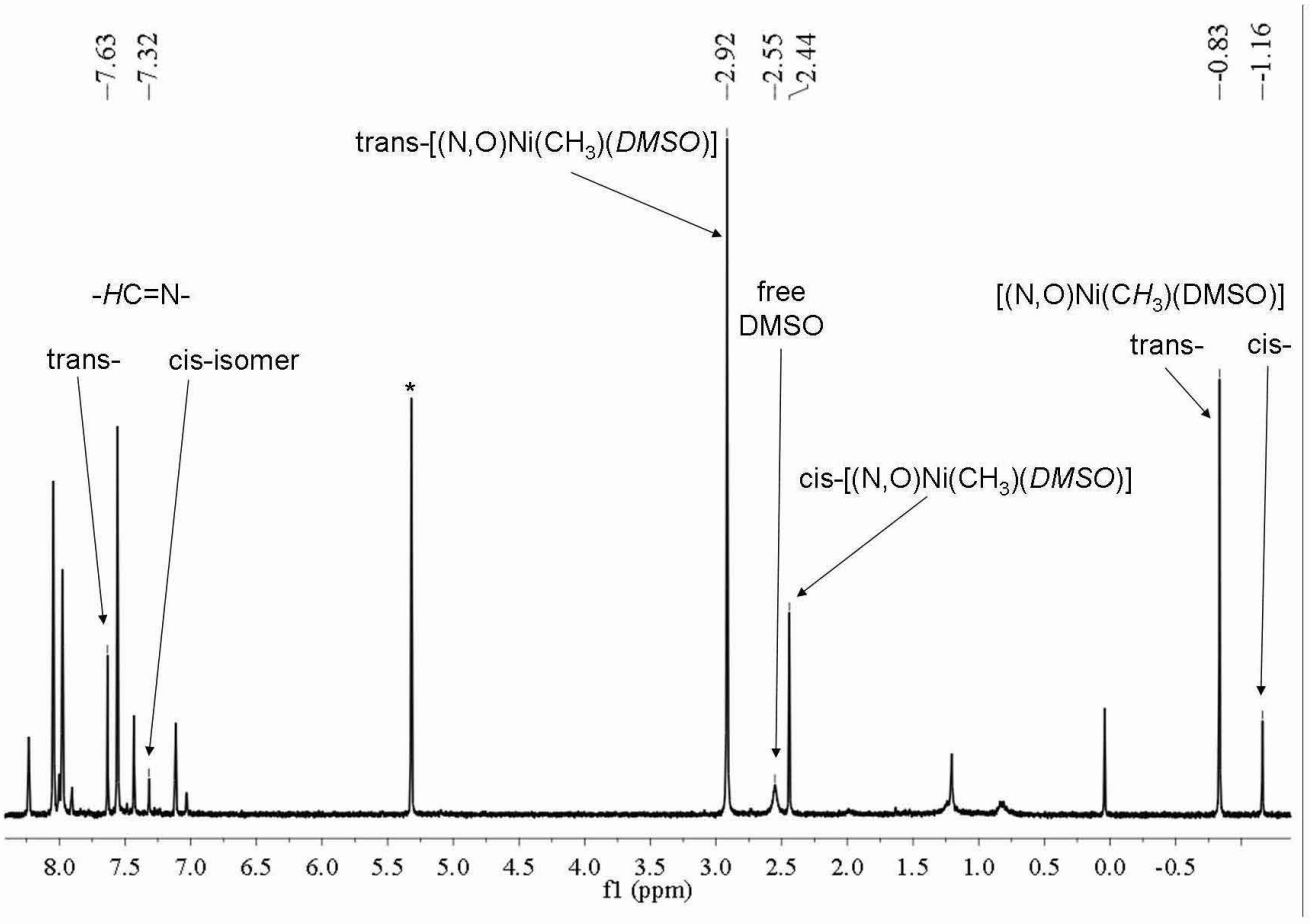

Figure S1. ^{1}H NMR spectrum of **1-DMSO** in CD_2Cl_2 (*) at -20°C.

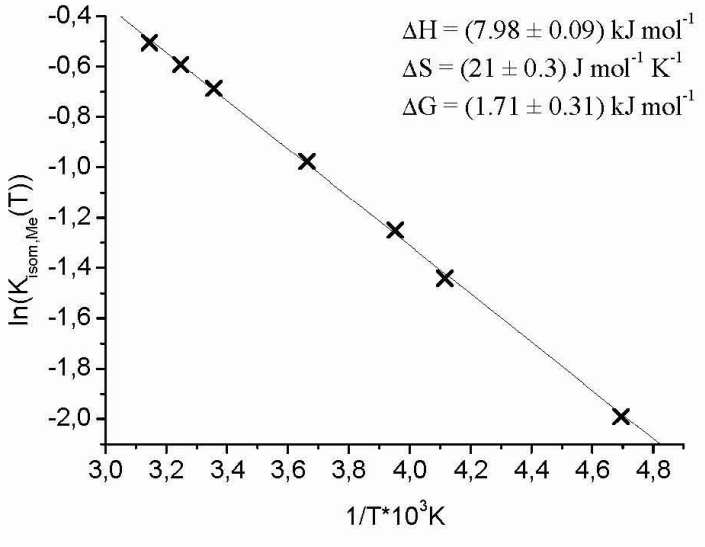

Figure S2. Van't Hoff plot of the equilibrium between the *trans* and *cis* isomer of **1-DMSO** in CD_2Cl_2 solution at variable temperatures.

Second-order rates of exchange of free with coordinated DMSO were determined for the *cis* and *trans* isomer separately by variable temperature ^{1}H NMR spectroscopy.[1] A CD_2Cl_2 solution of **1-DMSO** (7.7 mM) was prepared, to which 2.3 equivalents of DMSO (17.6 mM) were added. Coalescence of the resonances of coordinated and free DMSO was observed at 10°C for the *cis* isomer and was estimated to occur at 40 to 45°C in case of the *trans* isomer. Second-order exchange rates at coalescence temperatures were calculated according to $k(T_{coal.})_{exch.,DMSO} = \pi \cdot (\Delta\delta)/\{2^{1/2} \cdot [DMSO]\}$ ($\Delta\delta$ chemical shift difference between free and coordinated DMSO in Hz).[2] Rate constants at temperatures where the exchange occurs slowly on the chemical shift time scale were determined by comparison of peak widths at half heights of the resonances of coordinated DMSO in the presence and absence of excess DMSO according to $k(T)_{exch.,DMSO} = \pi \cdot (\Delta\nu)/[DMSO]$ ($\Delta\nu$ difference in line width at half height of the resonance of coordinated DMSO in Hz in the presence and absence of free DMSO). Activation parameters of DMSO exchange were obtained from linear regression of Eyring plots, $\ln(k(T)_{exch.,DMSO}/T)$ vs. 1/T (Figure S3).

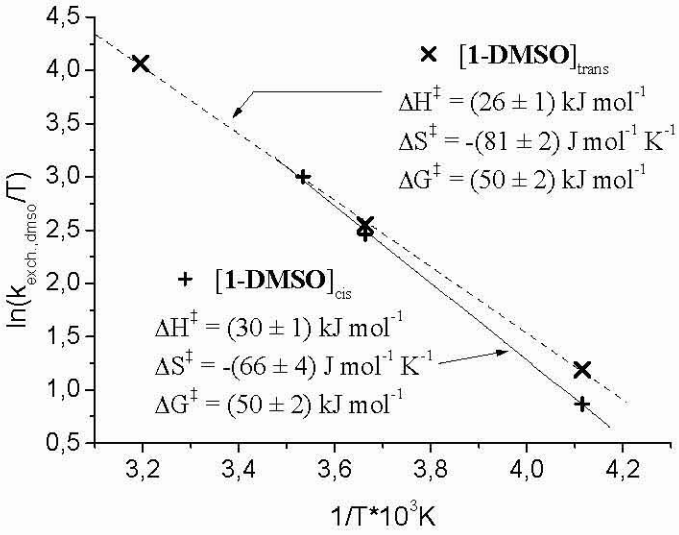

Figure S3. Eyring plots of temperature dependent rates of exchange of free (2.3 equivalents per Ni(II)-methyl) with coordinated DMSO for complex **1-DMSO**, determined by variable temperature ^{1}H NMR spectroscopy in CD_2Cl_2.

Reactivity of 1-DMSO towards methanol-d_4. Figure S4 depicts the ^{1}H NMR spectrum of a 17 mM solution of **1-DMSO** in methanol-d_4 (*) at 0°. ^{1}H and $^{13}C\{^1H\}$ NMR spectroscopic characterization of the resulting neutral Ni(II)-methyl species was carried out at 0°C to suppress the undesired methanolysis reaction. ^{1}H NMR (CD_3OD, 400 MHz, 0°C): δ 8.29 (br s, 4H, H15, 21, 23, 29); 8.12 (br s, 2H, H18, 26); 7.88 (d, $^4J_{H\text{-}H}$ = 2.3 Hz, 1H, H4); 7.66 (s, 1H, H7); 7.54 (m, 3H, H10, 11, 12); 7.17 (d, $^4J_{H\text{-}H}$ = 2.3 Hz, 1H, H6); 2.67 (s, 6H, DMSO); -1.28 (s, 3H, Ni-CH_3) ppm. ^{13}C NMR (CD_3OD, 100 MHz, 0°C): δ 170.2 (C7); 163.9 (C2); 151.7 (C8); 150.9 (C4); 142.9 (C14, 22); 142.8 (C6); 134.5 (C9, 13); 132.9 (q, $^2J_{C\text{-}F}$ = 33 Hz, C16, 19, 24, 27); 132.1 (C10, 12); 132.0 (C15, 21, 23, 29); 128.4 (C11); 125.1 (q, $^1J_{C\text{-}F}$ = 273 Hz, C17, 20, 25, 28); 122.5 (q, $^3J_{C\text{-}F}$ = 4 Hz, C18, 26); 122.1 (C1); 96 (C5); 73.1 (C3); 40.4 (DMSO); -14.0 (Ni-CH_3) ppm.

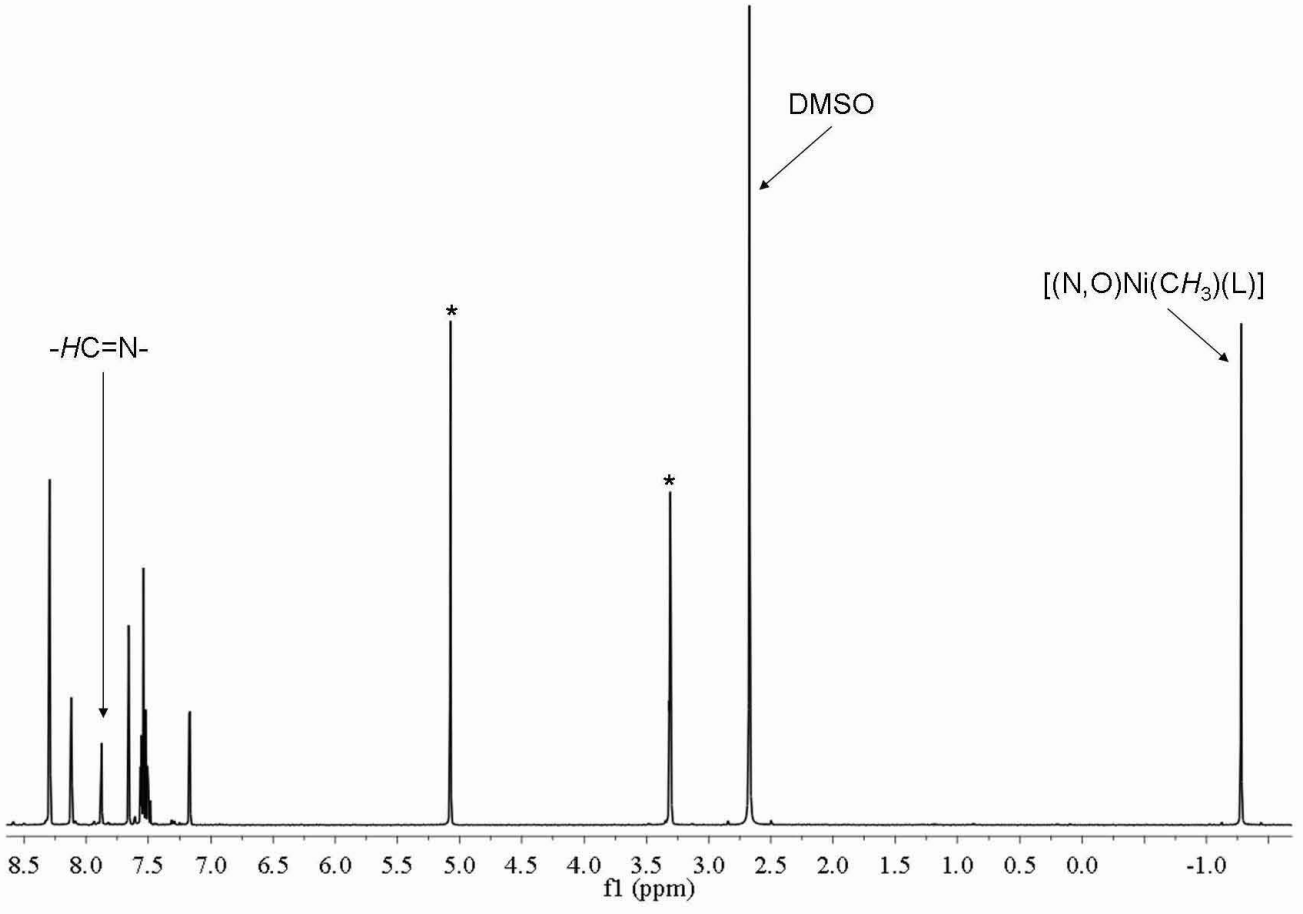

Figure S4. Representative ^{1}H NMR spectrum of **1-DMSO** in methanol-d_4 (*) solution at 0°C (L = DMSO, D_3COD).

A 15 mM methanol-d_4 solution was prepared from **1-DMSO** at room temperature in a glove box and the NMR tube was sealed with a rubber septum. The sample was transferred to the prewarmed NMR probe and the decrease of the Ni(II)-CH_3 resonance was monitored over four half life times. A first-order rate constant was determined from linear regression of a plot of $\ln([\text{Ni(II)-C}H_3]_t/[\text{Ni(II)-C}H_3]_{t=0})$ versus time (Figure S5). Dark red crystals separated from a light yellow methanol solution after the complete decomposition of the sample. An X-ray crystallographic analysis confirmed the formation of the bis-chelated Ni(II) complex *trans*-$[(N,O)_2Ni]$ but the crystal quality was poor in order to perform a detailed structural analysis of bond distances and angles. Unit cell parameters were determined as follows: Laue symmetry P-1, Z = 2; a = 11.3653(13)Å; b = 11.8194(13) Å; c = 21.682(2) Å; α = 91.559(9)°; β = 90.275(9)°; γ = 97.874(9)°; V = 2883.9(6) Å^3 (STOE IPDS II Image plate diffractometer, Mo-Kα radiation λ = 0.71073Å)

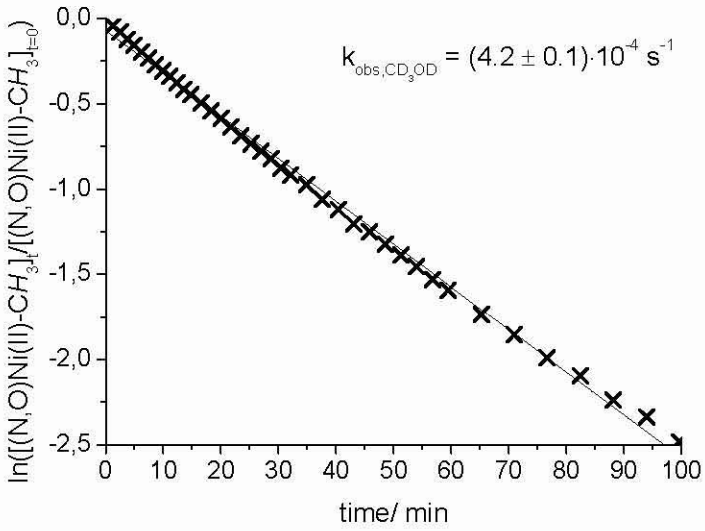

Figure S5. Representative first order plot of the time dependent decrease of the Ni(II)-CH_3 resonance in methanol-d_4 solution at 40°C.

Characterization of Ni(II)-ethyl complex 2-DMSO.

Figure S6 depicts a representative ^{1}H NMR spectrum (25°C) of a 3:1 mixture of Ni(II)-ethyl and Ni(II)-methyl (-1.19 ppm) complexes prepared from bubbling ethylene through a 14 mM solution of **1-DMSO** in DMSO-d_6 at 55°C for 45 minutes (cf. Experimental Section). The methylene and methyl protons of **2-DMSO** are assigned as α (-0.42 ppm) and β (-0.07 ppm), respectively. The rate of *cis-trans* isomerization of **2-DMSO** was estimated from the ^{1}H NMR spectra to be in the range of 2 -7 s^{-1}. Figure S7 shows the enlargement of the aromatic region of the ^{1}H NMR spectrum. The resonances of the aromatic protons 1- and 2-H4, 1- and 2-H6 and the imine resonances 2-H7 and 1-H7 are assigned.

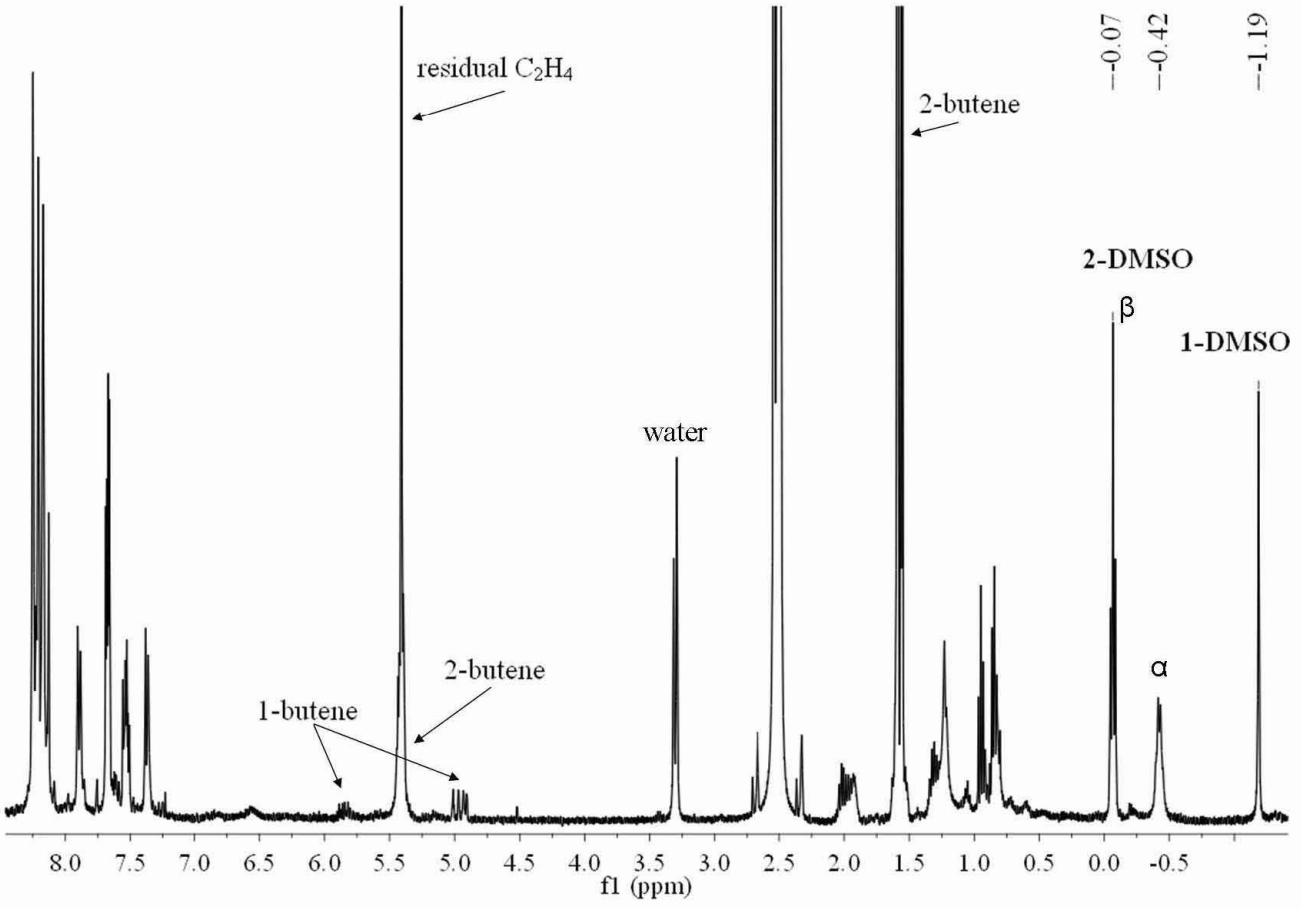

Figure S6. ^{1}H NMR spectrum of a 3:1 mixture of **2-DMSO** and **1-DMSO** in DMSO-d_6 at 25°C, obtained from bubbling ethylene through a solution of **1-DMSO**.

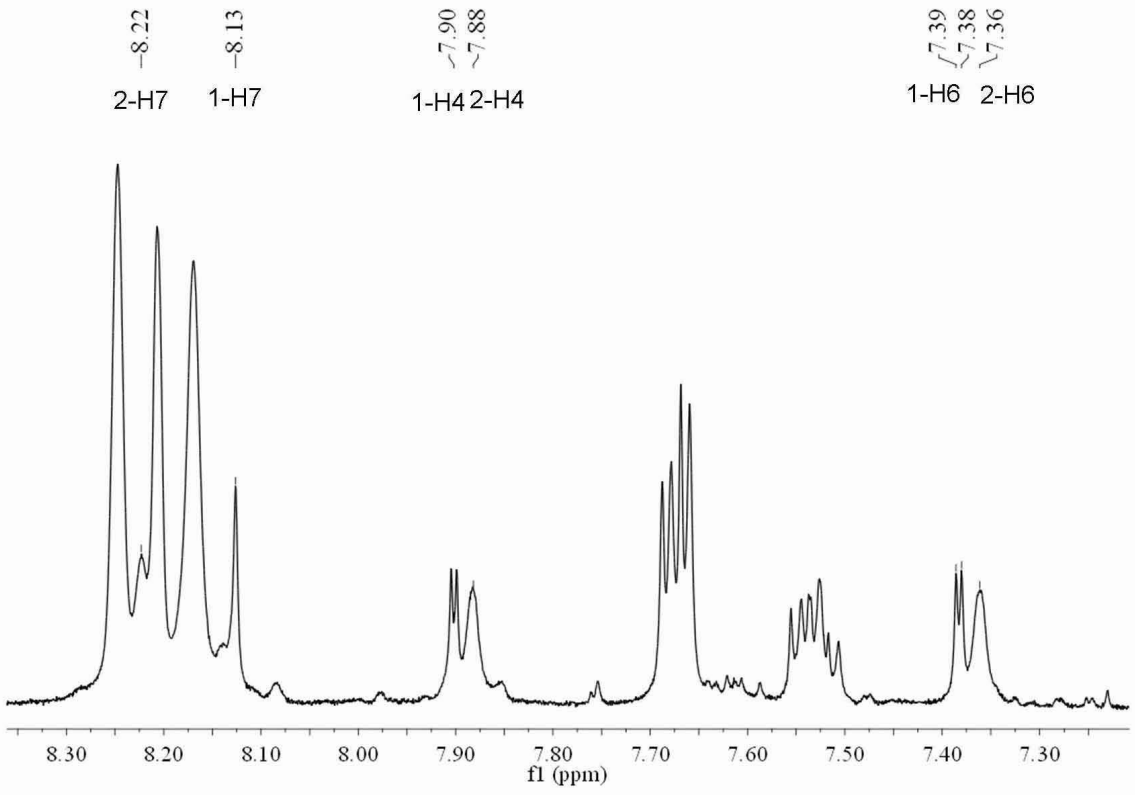

Figure S7. Expansion of the aromatic region of the ^{1}H NMR spectrum in Figure S6.

The alkane region of a ^{1}H NMR spectra of a sample containing **2_d-DMSO** and **1-DMSO** (1:1 ratio) in the absence (top) and presence (bottom) of water (H_2O) after ca. 24 h at room temperature is shown in Figure S8. The formation of 1,1,1,2,2-pentadeuteropropane $H_3CCD_2CD_3$, C_2H_6, CH_4 and CH_3D as the ultimate decomposition products of the neutral Ni(II)-alkyls is shown. A multiplet resonance at 0.74 ppm might correspond to ethane-h_1, the hydrolysis product of **2_d-DMSO**.

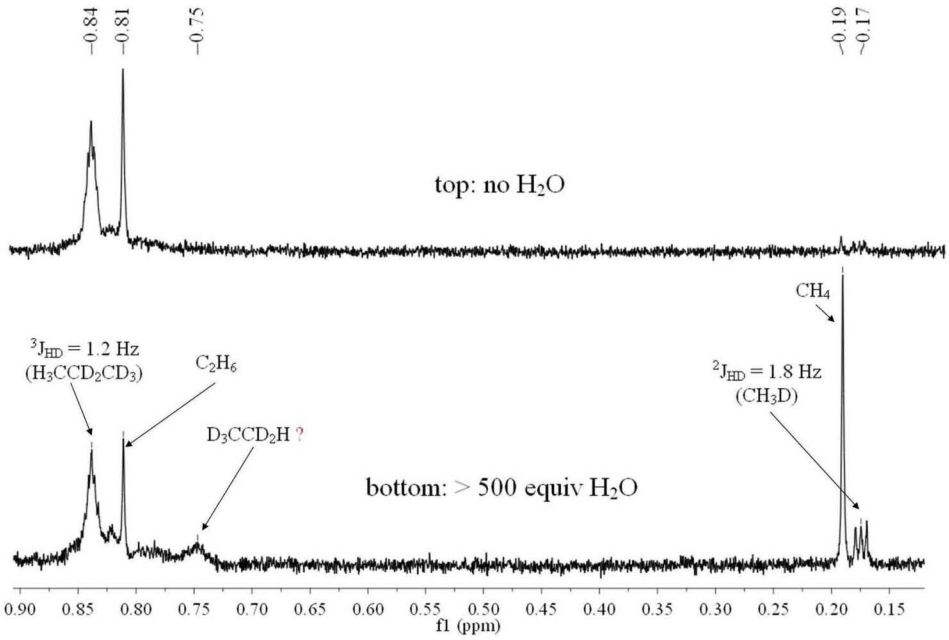

Figure S8. ^{1}H NMR spectrum (alkane region) showing the decomposition products from a mixture of the Ni(II)-alkyls **2_d-DMSO** and **1-DMSO** (1:1) in DMSO-d_6 after 24 h at 25°C.

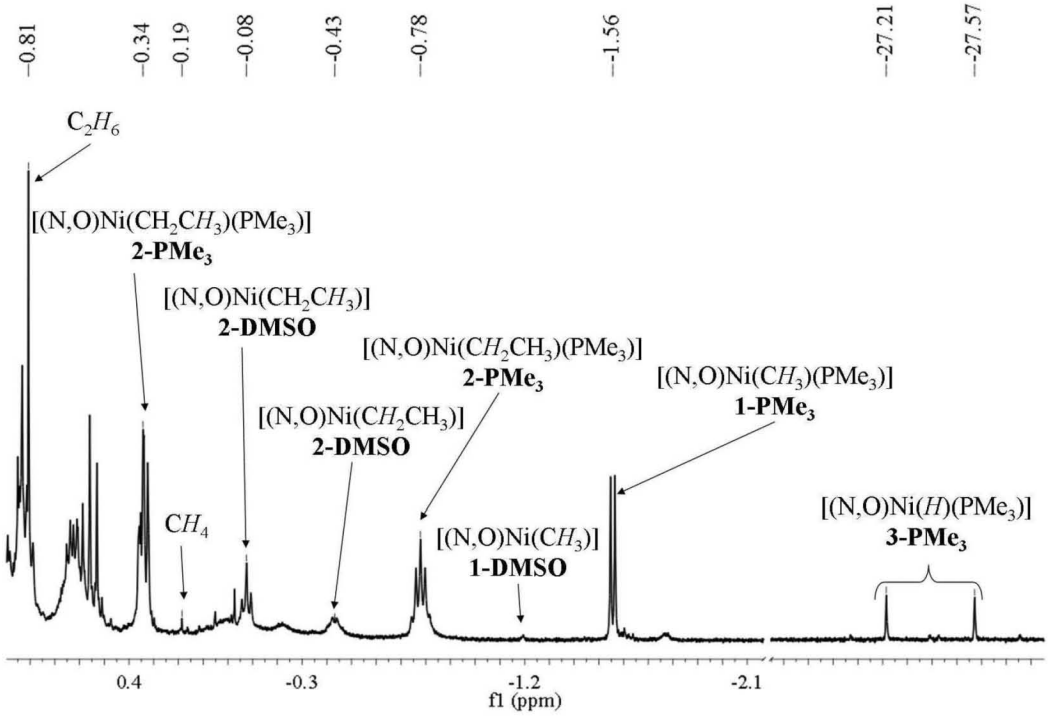

Figure S9. ^{1}H NMR spectrum showing the formation of the ultimate decomposition products ethane and methane from a mixture of Ni(II)-alkyls in the presence of the Ni(II)-hydride complex **3-PMe$_3$** in DMSO-d_6 after 12 h at 25°C (chemical shifts δ are assigned).

The gradual formation of ethane was also observed from a neat sample of **2-PMe$_3$** in THF-d_8 solution, prepared in situ from **3-PMe$_3$** with C_2H_4 at -10°C, as depicted in Figure S10. Notably, the chemical shifts of the Ni-*ethyl* fragment observed in THF-d_8 solution (T = -10°C) differ from that in DMSO-d_6 solution (T = 25°C).

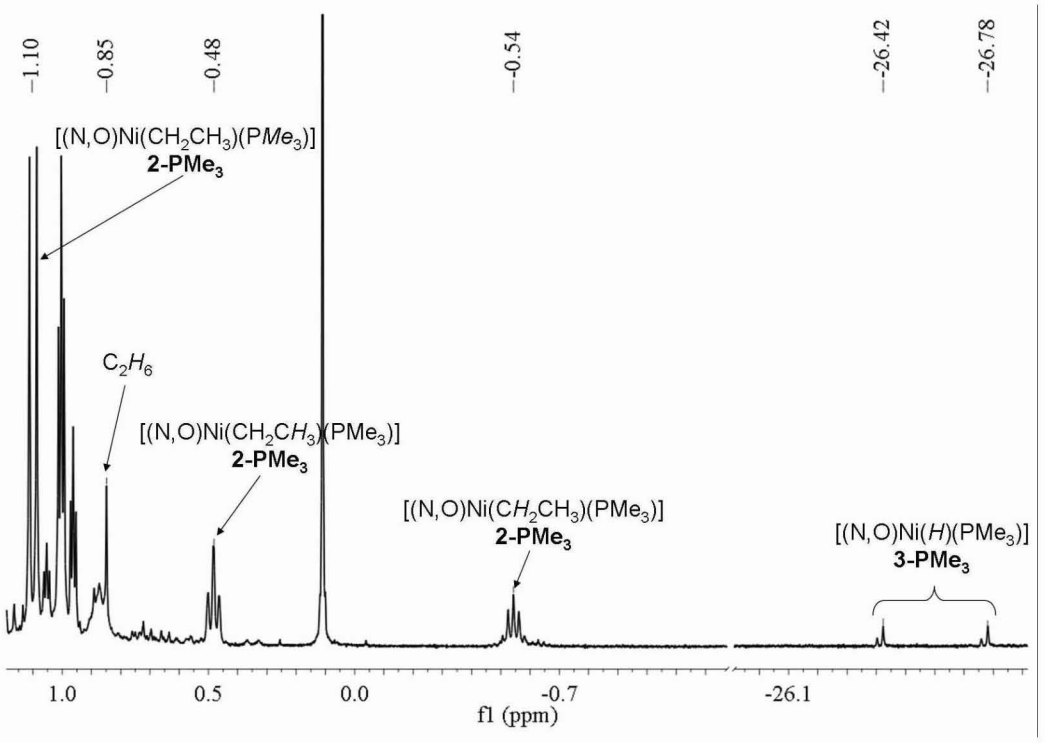

Figure S10. ^{1}H NMR spectrum showing the formation of ethane from **2-PMe$_3$** in THF-d_8 solution at -10°C (chemical shifts δ are assigned).

NMR-Scale Experiments at Various Temperatures

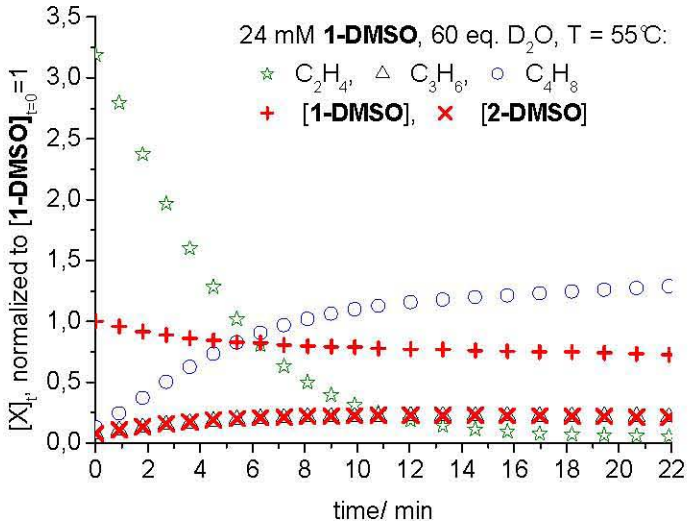

Figure S11. Typical time dependence of the conversion of **1-DMSO** into **2-DMSO**, the consumption of ethylene and the evolution of propene and butenes in the presence of D_2O. Relative concentrations of all Ni(II)-alkyl species and olefins are normalized to **1-DMSO** = 1 at t = 0. (24 mM **1-DMSO** in DMSO-d_6, 60 equiv. D_2O, T = 55°C).

Kinetic analysis of ethane formation from 1-DMSO.

Second-order rate constants of the bimolecular elimination of ethane from **1-DMSO** were determined from linear regression of plots of $1/[\mathbf{1\text{-}DMSO}]_t - 1/[\mathbf{1\text{-}DMSO}]_{t=0}$ versus time. Representative kinetic plots are shown in Figure S12. Error margins given are the estimated standard deviations (esd) calculated from the linear regression to the dataset. Since the reaction proceeds very slowly at 55°C only one half life time was followed, whereas at 80°C the reaction was monitored for 2 ½ half life times.

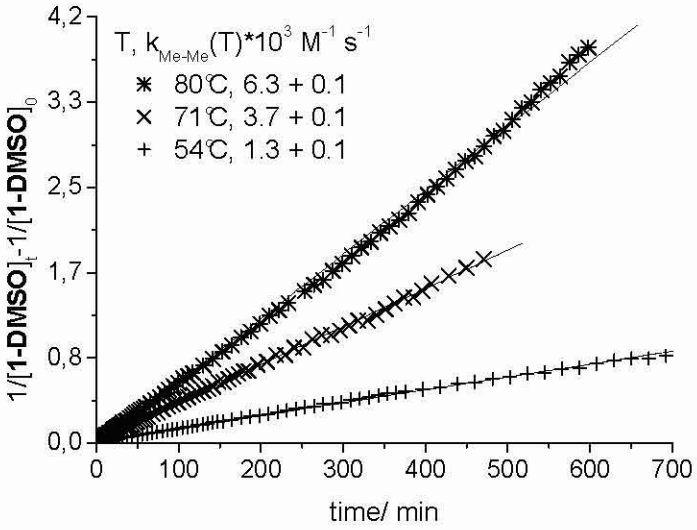

Figure S12. Second-order plots of decomposition of **1-DMSO** to ethane monitored by ^{1}H NMR spectroscopy at variable temperatures in DMSO-d_6 solution.

Kinetic analysis of methane formation from 1-DMSO and 3-PMe$_3$.

Second-order rate constants of the bimolecular elimination of methane from **1-DMSO** and **3-PMe$_3$** were determined from linear regressions of plots of $1/\{[\mathbf{3\text{-}PMe_3}]_{t=0}\text{-}[\mathbf{1\text{-}DMSO}]_{t=0}\}*\ln\{[\mathbf{3\text{-}PMe_3}]_t*[\mathbf{1\text{-}DMSO}]_{t=0}/\{[\mathbf{3\text{-}PMe_3}]_{t=0}*[\mathbf{1\text{-}DMSO}]_t\}\}$ versus time. Representative kinetic plots are shown in Figure S13. Error margins given are the estimated standard deviations (esd) calculated from the linear regression to the dataset. The reaction proceeds slowly for temperatures T < 20°C. Therefore, the decrease of **1-DMSO** was monitored for one half life time only. At temperatures T > 20°C the disappearance of **1-DMSO** was followed for two half life times. After ca. 2 half life times a strong broadening of all resonances was observed that limited the accuracy of the integration. A black precipitate, presumably Ni black, separated out from the reaction solution.